International Geology Review
Publication details, including instructions for authors and subscription information:
http://www.tandfonline.com/loi/tigr20

Petrogenesis of adamellites from eastern Shandong Province: geochronological, geochemical, and Sr-Nd-Pb isotopic evidence

Tao Wang[ab], Shen Liu[c], Jiaxi Zhou[b] & Yubin Li[d]

[a] College of Earth Sciences, Chengdu University of Technology, Chengdu 610059, China

[b] State Key Laboratory of Ore Deposit Geochemistry, Institute of Geochemistry, Chinese Academy of Sciences, Guiyang 550002, China

[c] Department of Geology, Northwest University, Xian 710127, China

[d] No. 5 Geological Party, Tibet Bureau of Geology and Mineral Exploration and Development, Golmud 816000, China

Published online: 13 May 2013.

To cite this article: Tao Wang, Shen Liu, Jiaxi Zhou & Yubin Li (2013) Petrogenesis of adamellites from eastern Shandong Province: geochronological, geochemical, and Sr-Nd-Pb isotopic evidence, International Geology Review, 55:14, 1786-1800, DOI: 10.1080/00206814.2013.796077

To link to this article: http://dx.doi.org/10.1080/00206814.2013.796077

International Geology Review, 2013
Vol. 55, No. 14, 1786–1800, http://dx.doi.org/10.1080/00206814.2013.796077

Taylor & Francis
Taylor & Francis Group

Petrogenesis of adamellites from eastern Shandong Province: geochronological, geochemical, and Sr–Nd–Pb isotopic evidence

Tao Wang[a,b]*, Shen Liu[c], Jiaxi Zhou[b] and Yubin Li[d]

[a]*College of Earth Sciences, Chengdu University of Technology, Chengdu 610059, China;* [b]*State Key Laboratory of Ore Deposit Geochemistry, Institute of Geochemistry, Chinese Academy of Sciences, Guiyang 550002, China;* [c]*Department of Geology, Northwest University, Xian 710127, China;* [d]*No. 5 Geological Party, Tibet Bureau of Geology and Mineral Exploration and Development, Golmud 816000, China*

(*Accepted 11 April 2013*)

Geochronology, geochemistry, and whole-rock Sr–Nd–Pb isotopes were studied on a suite of Mesozoic adamellites from eastern China to characterize their ages and petrogenesis. Sensitive high-resolution ion microprobe U–Pb zircon analyses were done, yielding consistent ages of 123.2 ± 1.8 to 122.1 ± 2.1 Ma for the samples. These rocks belong to the alkaline magma series in terms of $K_2O + Na_2O$ contents (8.45–9.58 wt.%) and to the shoshonitic series based on their high K_2O contents (5.23–5.79 wt.%). The adamellites are further characterized by high light rare earth element contents [$(La/Yb)_N$ = 14.96–45.99]; negative Eu anomalies ($\delta Eu = 0.46–0.75$); positive anomalies in Rb, Th, Pb, and U; and negative anomalies in Sr, Ba, and high field-strength elements (i.e. Nb, Ta, P, and Ti). In addition, all of the adamellites in this study display relatively low radiogenic Sr [$(^{87}Sr/^{86}Sr)_i = 0.7081–0.7089$] and negative $\varepsilon_{Nd}(t)$ values from –16.70 to –17.80. These results suggest that the adamellites were derived from low-degree partial melting of an enriched lithospheric mantle below the North China Craton (NCC). The parent magmas likely experienced fractional crystallization of potassium feldspar, plagioclase and Fe–Ti oxides (e.g. rutile, ilmenite, and titanite), apatite, and zircon during the ascent of alkaline rocks without crustal contamination.

Keywords: alkaline intrusions; enriched lithospheric mantle; crustal foundering; granite; petrogenesis; eastern Shandong Province

1. Introduction

Eastern Shandong Province is located in the Sulu high pressure (HP) to ultrahigh pressure (UHP) metamorphic belt, which is widely accepted as the eastern part of Qinling–Dabie collisional orogenic belt between the North China and Yangtze blocks (Huang 1978; Yin and Ni 1993; Xu and Zhu 1994; Wang *et al*. 1995; Cong 1996; Li *et al*. 2002; Zheng *et al*. 2002). It is generally deemed that alkaline rocks are emplaced in a non-orogenic, intraplate, or rift-related tectonic background (Yan *et al*. 2002), and mostly come from the upper mantle (Ren 2003). However, alkaline rocks may emplace in post-orogenic stages in a short interval of time, such as in the Permian–Triassic Western Mediterranean province (Bonin *et al*. 1987), Himalayan belt (Miller *et al*. 1999; Williams *et al*. 2004), Sulu Belt (Yang *et al*. 2005a,b), and other cases (Guo *et al*. 2005). The Jiazishan alkaline association in eastern Shandong Province has been reported upon (Chen *et al*. 2003; Yang *et al*. 2005a, 2005b). However, the origin of these rocks remains controversial (Yang *et al*. 2005a; Xie *et al*. 2006). Consequently, our study on the alkaline intrusions may furnish further constraints on this debate and probe the petrogenetic processes occurring during a later evolutionary stage. In this article, we provide petrographic, geochronological, geochemical, and Sr–Nd–Pb isotopic data on the alkaline intrusions from eastern Shandong Province. Their petrogenesis and tectonic implication are discussed from these data. This study will help us further reveal the properties of Mesozoic lithospheric mantle beneath the North China Craton (NCC), understand the regional tectonic evolution of the lithosphere, and limit the initial age and the mechanism of the lithosphere thinning.

2. Geological background and petrography

The NCC, Yangtze Craton, and Tan-Lu Fault are three representative tectonic units of eastern China. As a long-lived fault, the Tan-Lu Fault extends through Shandong Province and separates the Shandong region into parts. The Sulu terrain was offset to the north by sinistral movement on Tan-Lu Fault of about 500 km (Xu and Zhu 1994), where UHP metamorphic rocks, such as meta-granitoids

*Corresponding author. Email: wangtao10@cdut.cn

(Hirajima *et al*. 1990), politic schists (Zhang *et al*. 1995), ultramafics (Yang *et al*. 1993), marbles (Kato *et al*. 1997), and amphibolite facies granitic gneisses (Enami and Zang 1993); and voluminous syn-collisional and post-collisional magmatic rocks, such as adakites (Guo *et al*. 2006; Liu *et al*. 2008), gabbro (Meng *et al*. 2005; Liu *et al*. 2010), granitoids and diorite (Hong *et al*. 2003; Huang *et al*. 2005), mafic dikes (Yang *et al*. 2005b; Liu *et al*. 2012), and alkaline complexes (Guo *et al*. 2005; Yang *et al*. 2005a) are widespread. These UHP metamorphic rocks occur as sporadic lenticular bodies in the regional granitic gneisses. Abundant U–Pb zircon ages and the Sm–Nd isochron have documented that the continental collision and UHP metamorphism took place in the Early–Middle Triassic (240–220 Ma) (Chavagnac and Jahn 1996; Hacker *et al*. 1998; Zheng *et al*. 2002; Liu *et al*. 2004). Mesozoic magmatic rocks mainly formed between 225 and 114 Ma (Zhao *et al*. 1997; Zhou and Lu 2000; Fan *et al*. 2001; Zhou *et al*. 2003, 2013; Huang *et al*. 2005; Meng *et al*. 2005; Yang *et al*. 2005a; Guo *et al*. 2006; Liu *et al*. 2008, 2010, 2012). High-K calc-alkaline granitic rocks are widely distributed in the Sulu orogenic belt, and most of them formed in the Late Jurassic (160–150 Ma) and Early Cretaceous (130–125 Ma) (Wang *et al*. 1998; Zhang *et al*. 2003).

Based on the 1:50,000 regional geological map of Shandong Province, sampling locations of Mesozoic alkali-rich intrusive rocks were chosen in the central section of the Sulu terrain from Dadian to Junan (Figure 1A). The alkali-rich intrusive rocks are mainly adamellites. The Dadian adamellitic intrusion outcrops over approximately 560 km^2. It mainly intruded into Archaean to lower Proterozoic gneisses and is associated with Yanshanian granites (Figure 1B). The rocks are commonly light grey and medium- to coarse-grained with granular and porphyritic textures and blocky structure. They are dominated by diopside (8–10%), quartz (10–15%), andesine (30–35%), K-feldspar (40–45%), subordinate (2%) biotite and amphibole, and accessory minerals including zircon, apatite, titanite, and magnetite (DD1 and DD2). The Junan adamellite outcrops over approximately 130 km^2 and is similar to Dadian adamellite in terms of stratum, colour, texture, structure, and composition (JN).

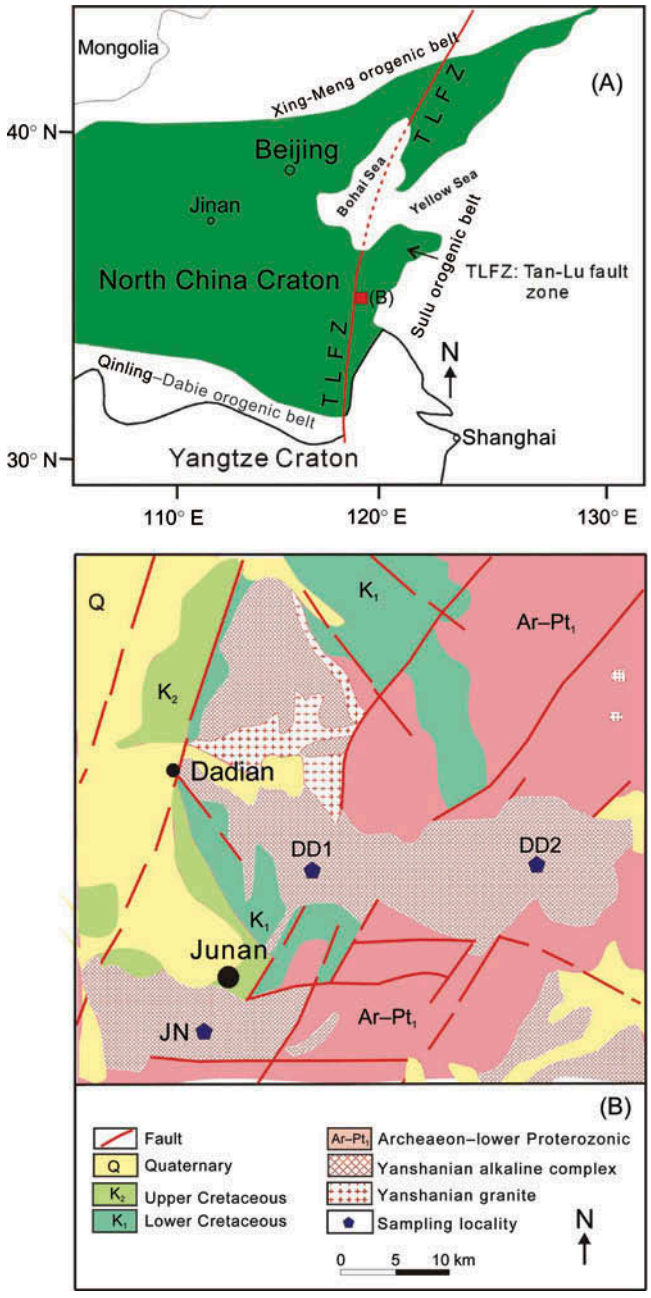

Figure 1. (A) Simplified tectonic map of the NCC. (B) Geological map of the study areas and the distributions of the adamellites throughout eastern Shandong Province, eastern China.

3. Analytical methods

3.1. Zircon SHRIMP U–Pb dating

Zircon U–Pb isotopic analyses were performed at the Chinese Academy of Geological Sciences (Beijing) using a sensitive high-resolution ion microprobe (SHRIMP-II). Sample preparation and basic operations have been described in detail by Compston *et al*. (1992) and Song *et al*. (2002). The $^{206}Pb/^{238}U$ ages are believed to be the most dependable, since the zircons are concordant and the low count rates on ^{207}Pb lead to large statistical uncertainties, making the $^{207}Pb/^{206}Pb$ and $^{207}Pb/^{235}U$ ratios less sensitive measures of age for younger zircons (Compston *et al*. 1992). The zircons were detached from four quartz monzonites. Representative zircon grains were handpicked under a binocular microscope, mounted in an epoxy resin disc, and then polished and coated with gold film. Zircons were documented with transmitted and reflected light micrographs as well as cathodoluminescence (CL) pictures to show their external and internal structures. The U–Pb isotope data were collected in sets of

five scans throughout the masses, and a reference zircon TEM (417 Ma) (Black *et al*. 2003) was analysed after every four samples. The uncertainties in ages are at the 1σ level, and the weighted mean ages are quoted at 95% or 2σ confidence.

3.2. *Major and trace elemental analyses*

Major elements were tested with a PANalytical Axios-advance (Axios PW4400) X-ray fluorescence spectrometer (XRF) at the State Key Laboratory of Ore Deposit Geochemistry, Institute of Geochemistry, Chinese Academy of Sciences (IGCAS). Fused glass discs were used and the analytical precision as determined on the Chinese National standard GSR-1 and GSR-3 was better than 5%. Loss on ignition (LOI) was gained by 1 g powder heated up to 1100°C for 1 h.

Trace elements were analysed with a POEMS ICP-MS at the National Research Center of Geoanalysis, Chinese Academy of Geosciences. The powdered samples (50 mg) were dissolved in high-pressure Teflon bombs using a HF + HNO_3 mixture for 48 h at approximately 190°C (Qi *et al*. 2000). Rh was used as an internal standard to monitor signal drift during counting. The international standard, GBPG-1, was used for analytical quality control. The analytical precision was generally better than 5% for all elements. Analyses of international standards OU-6 and GBPG-1 are in agreement with recommended values.

3.3. *Sr–Nd–Pb isotopic analyses*

Whole-rock Sr–Nd–Pb isotopic data were obtained using a Finnigan MAT-262 thermal ionization mass spectrometer (TIMS) at the Isotopic Geochemistry Laboratory of the Yichang Institute of Geology and Mineral Resources. For Rb–Sr and Sm–Nd isotope analyses, sample powders were spiked with mixed isotope tracers, dissolved in Teflon capsules with HF + HNO_3 acids, and separated using the conventional cation-exchange technique. Procedural blanks were <200 pg for Sm and Nd, and <500 pg for Rb and Sr. The mass fractionation corrections for Sr and Nd isotopic ratios were based on $^{86}Sr/^{88}Sr = 0.1194$ and $^{146}Nd/^{144}Nd = 0.7219$, respectively. Analyses of standards during the period of analysis are as follows:

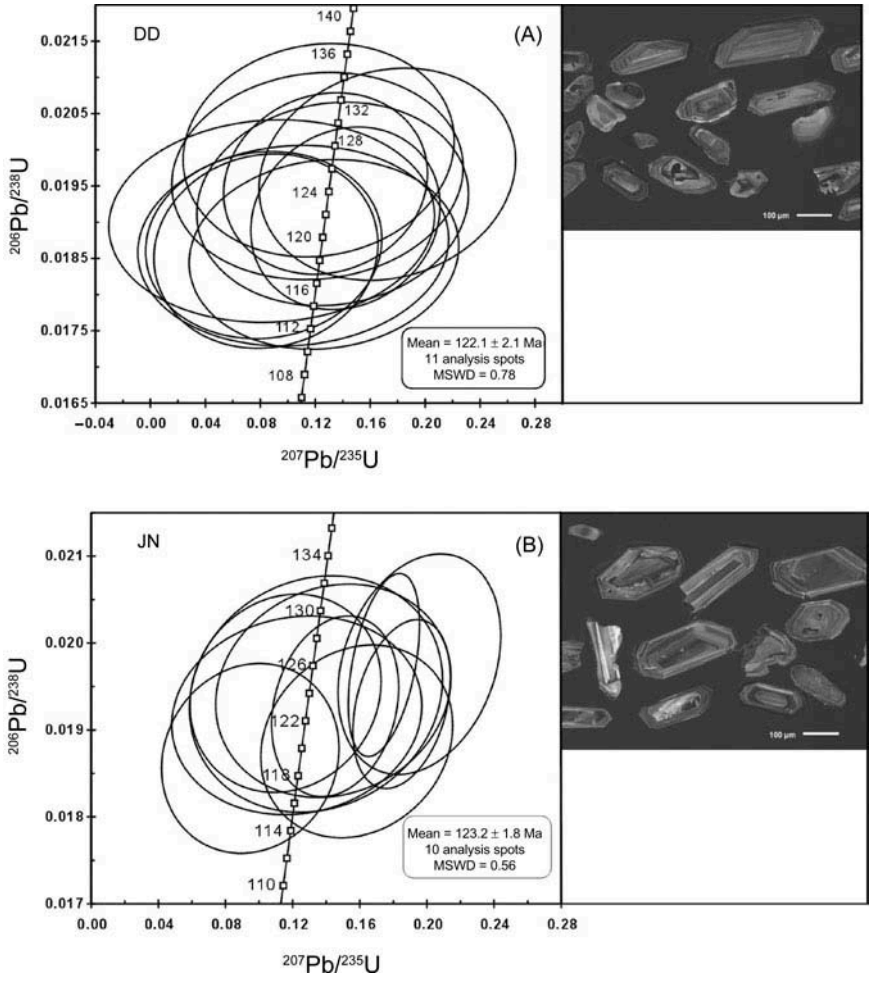

Figure 2. SHRIMP zircon U–Pb Concordia diagrams for the adamellites from eastern Shandong Province: (A) DD and (B) JN.

NBS987 gave $^{87}Sr/^{86}Sr = 0.710246 \pm 16(2\sigma)$; La Jolla gave $^{143}Nd/^{144}Nd = 0.511863 \pm 8\ (2\sigma)$. Pb was separated and purified using the conventional cation-exchange technique (AG1 × 8200–400 resin) with diluted HBr as eluent. Analyses of NBS981 during the period of analysis yielded $^{204}Pb/^{206}Pb = 0.0896 \pm 15$, $^{207}Pb/^{206}Pb = 0.91446 \pm 80$, and $^{208}Pb/^{206}Pb = 2.16171 \pm 200$.

4. Results

4.1. Zircon U–Pb geochronology

Sufficient and euhedral zircon grains were selected from the adamellites (DD1, DD2, and JN) for the analysis. The grains are colourless, transparent, and mostly elongate-prismatic, showing prismatic form with magmatic oscillatory zoning under CL excitation. Selected zircon CL pictures are given in Figure 2. The U–Pb zircon dates for these samples are presented in Table 1. The zircon samples have variable abundances of U (133–346 ppm), Th (178–733 ppm), and Th/U(1.29–2.12), further showing a mamatic origin for these zircons. SHRIMP U–Pb dating of 11 and 10 zircon grains with oscillatory structures were concordant and yielded weighted mean $^{206}Pb/^{238}Pb$ ages of 122.1 ± 2.1 and 123.2 ± 1.8 million years (95% confidence interval, Figures 2A and 2B). These ages were interpreted as the crystallization ages of samples DD1, DD2, and JN.

4.2. Major and trace elemental geochemical characteristics

The major element concentrations for the studied adamellites are listed in Table 2. The adamellites show a range in SiO_2 values from 61.09 to 64.25 wt.% and are relatively high in total alkali contents ($K_2O + Na_2O$ = 8.93–10.08 wt.%), with K_2O = 5.23–5.79 wt.% and Na_2O = 3.65–4.41 wt.%. All samples plot in the alkaline fields on the total alkali–silica (TAS) diagram (Figure 3A). Moreover, the rocks also straddle the alkaline series in the SiO_2 *versus* AR graph (Figure 3B) of Wright (1969). In the plot of Na_2O *versus* K_2O (Figure 4A), the adamellites belong to the shoshonitic series. Figure 4B shows the composition of the rocks in terms of their molar ratios of $Al_2O_3/(CaO + K_2O + Na_2O)$ and $Al_2O_3/(K_2O + Na_2O)$; they are all metaluminous. All rocks of the adamellites display regular trends of decreasing CaO, MgO, Fe_2O_3, P_2O_5,TiO_2, Al_2O_3, Sr, and Ba with increasing SiO_2, whereas weak correlations are observed in the plots of SiO_2 *versus* K_2O, Na_2O, Zr, and Rb (Figures 5 and 6). In the 10,000 * Ga/Al *versus* $K_2O + Na_2O$ and Zr discrimination diagrams (Figure 7) of Whalen *et al.* (1987), the samples are all classified as A-type granite.

The trace element compositions of the samples are presented in Table 3. Total rare earth element (REE) ranges from 296 to 765 ppm. The chondrite-normalized REE

Table 1. SHRIMP U–Pb isotopic data for zircon within the adamellites from eastern Shandong Province.

Spot	U (ppm)	Th (ppm)	Pb (ppm)	Th/U	$^{206}Pb/^{238}U$ (Ma)	$^{207}Pb/^{206}Pb$	±1 (%)	$^{207}Pb/^{235}U$	±1 (%)	$^{206}Pb/^{238}U$	±1 (%)
DD											
1.1	170	212	2.82	1.29	118.5	0.0490	32	0.1260	32	0.0186	3
2.1	163	215	2.75	1.36	119.3	0.0320	43	0.0820	43	0.0187	3
3.1	148	202	2.47	1.42	121.7	0.0540	20	0.1420	20	0.0191	3
4.1	154	218	2.62	1.46	122.9	0.0500	30	0.1330	30	0.0193	3
5.1	145	248	2.45	1.78	118.8	0.0330	40	0.0840	40	0.0186	3
6.1	138	178	2.37	1.33	125.5	0.0640	22	0.1720	22	0.0197	3
7.1	226	292	3.79	1.34	119.3	0.0400	44	0.1040	44	0.0187	3
8.1	175	233	3.00	1.36	121.4	0.0340	55	0.0880	55	0.0190	3
9.1	133	178	2.34	1.38	125.4	0.0450	36	0.1220	36	0.0196	3
10.1	161	203	2.86	1.30	127.6	0.0440	33	0.1220	33	0.0200	3
11.1	193	280	3.34	1.50	124.7	0.0470	24	0.1270	24	0.0195	3
JN											
1.1	231	299	3.89	1.33	122.4	0.0460	25	0.1220	25	0.0192	2
2.1	144	257	2.47	1.85	126.1	0.0718	10	0.1960	10	0.0198	3
3.1	202	298	3.43	1.53	124.2	0.0540	20	0.1440	20	0.0195	3
4.1	346	733	5.77	2.19	123.2	0.0695	6	0.1850	6	0.0193	2
5.1	199	347	3.42	1.80	124.0	0.0432	20	0.1160	20	0.0194	2
6.1	322	650	5.33	2.08	119.3	0.0368	23	0.0950	23	0.0187	2
7.1	254	397	4.32	1.61	126.1	0.0640	5	0.1744	5	0.0198	2
8.1	145	199	2.49	1.41	124.0	0.0500	23	0.1340	23	0.0194	3
9.1	239	350	3.92	1.52	120.5	0.0680	15	0.1580	15	0.0189	2
10.1	265	505	4.47	1.97	123.1	0.0547	10	0.1450	11	0.0193	2

Table 2. Whole-rock major element compositions (wt.%) of the representative adamellites from eastern Shandong Province.

Sample	Rock type	SiO_2	Al_2O_3	TiO_2	Fe_2O_3	MnO	MgO	CaO	Na_2O	K_2O	P_2O_5	LOI	Total	$Mg^{\#}$
DC1-1	Adamellite	60.29	16.05	0.71	5.36	0.10	2.23	3.89	3.78	5.15	0.35	2.61	100.52	37.20
DC1-2	Adamellite	61.41	16.35	0.74	5.74	0.11	2.33	4.09	3.79	5.35	0.37	0.11	100.39	36.63
DC1-3	Adamellite	63.77	15.79	0.64	4.87	0.10	1.91	3.13	3.78	5.79	0.29	0.32	100.40	35.83
DC1-4	Adamellite	60.88	16.45	0.74	5.65	0.12	2.33	4.05	3.88	5.38	0.38	0.08	99.93	36.99
DC1-5	Adamellite	60.75	16.30	0.75	5.75	0.11	2.39	4.14	3.79	5.31	0.38	0.13	99.79	37.18
DC1-6	Adamellite	61.01	16.32	0.76	5.99	0.13	2.44	4.14	3.81	5.35	0.39	0.14	100.48	36.71
DC1-7	Adamellite	60.77	16.31	0.75	5.81	0.11	2.47	4.11	3.69	5.37	0.38	0.34	100.11	37.71
DC1-8	Adamellite	62.50	15.84	0.72	6.28	0.14	2.17	3.76	3.73	5.28	0.35	0.07	100.84	32.97
DC1-9	Adamellite	60.73	16.35	0.75	5.70	0.11	2.34	4.13	3.79	5.39	0.37	0.27	99.93	36.89
DC2-1	Adamellite	62.38	15.73	0.68	5.29	0.11	2.20	3.68	3.83	5.34	0.42	0.28	99.94	37.19
DC2-2	Adamellite	62.53	15.35	0.69	5.28	0.11	2.44	3.87	3.74	5.44	0.45	0.06	99.96	39.68
DC2-3	Adamellite	61.15	15.65	0.74	5.60	0.11	2.57	4.06	3.90	5.12	0.47	0.47	99.85	39.52
DC2-4	Adamellite	61.88	16.13	0.70	5.47	0.12	2.39	3.81	4.04	5.38	0.46	0.12	100.50	38.35
DC2-5	Adamellite	62.04	16.07	0.73	5.38	0.11	2.34	3.78	3.89	5.61	0.44	0.13	100.51	38.24
DC2-6	Adamellite	61.05	16.09	0.75	5.70	0.11	2.51	4.03	3.94	5.23	0.43	0.04	99.87	38.54
DC2-7	Adamellite	62.11	15.81	0.70	5.26	0.11	2.30	3.71	3.92	5.32	0.43	0.14	99.81	38.37
DC2-8	Adamellite	62.13	16.11	0.60	5.41	0.11	2.35	3.73	3.95	5.53	0.44	0.04	100.39	38.21
DC2-9	Adamellite	62.24	15.89	0.72	5.39	0.11	2.43	3.74	3.89	5.46	0.44	0.06	100.37	39.09
JN-1	Adamellite	63.54	15.59	0.58	5.03	0.11	2.07	3.40	3.59	5.42	0.31	0.21	99.83	36.95
JN-2	Adamellite	62.52	15.56	0.63	5.28	0.11	2.22	3.63	3.63	5.28	0.32	0.62	99.81	37.45
JN-3	Adamellite	63.24	15.80	0.62	5.10	0.10	2.08	3.61	3.67	5.25	0.31	0.18	99.96	36.74
JN-4	Adamellite	64.25	14.93	0.64	5.38	0.10	2.12	3.16	3.38	5.69	0.31	0.07	100.02	35.94
JN-5	Adamellite	63.62	14.59	1.11	5.59	0.11	2.22	3.64	3.36	5.33	0.32	0.29	100.19	36.12
JN-6	Adamellite	63.49	15.99	0.55	5.64	0.12	2.06	3.65	3.81	5.26	0.31	0.03	100.91	34.21
JN-7	Adamellite	63.95	15.50	0.63	4.81	0.09	1.95	3.45	3.63	5.38	0.29	0.28	99.97	36.60
JN-8	Adamellite	62.64	16.23	0.69	5.52	0.10	2.33	3.94	3.46	5.28	0.35	0.12	100.66	37.54
GSR1	RV*	72.83	13.40	0.29	2.14	0.06	0.42	1.55	3.13	5.01	0.09	0.70	99.62	
GSR1	MV*	72.65	13.52	0.29	2.18	0.06	0.46	1.56	3.25	5.03	0.11	0.69	99.80	
GSR3	RV*	44.64	13.83	2.37	13.40	0.17	7.77	8.81	3.38	2.32	0.95	2.24	99.88	
GSR3	MV*	44.75	14.14	2.36	13.35	0.16	7.74	8.82	3.18	2.30	0.97	2.12	99.89	

Note: LOI, loss on ignition; $Mg^{\#} = 100 \times Mg/(Mg + \sum Fe)$ atomic ratio; RV*, recommended values; MV*, measured values; values for GSR-1 and GSR-3 are from Wang *et al.* (2003).

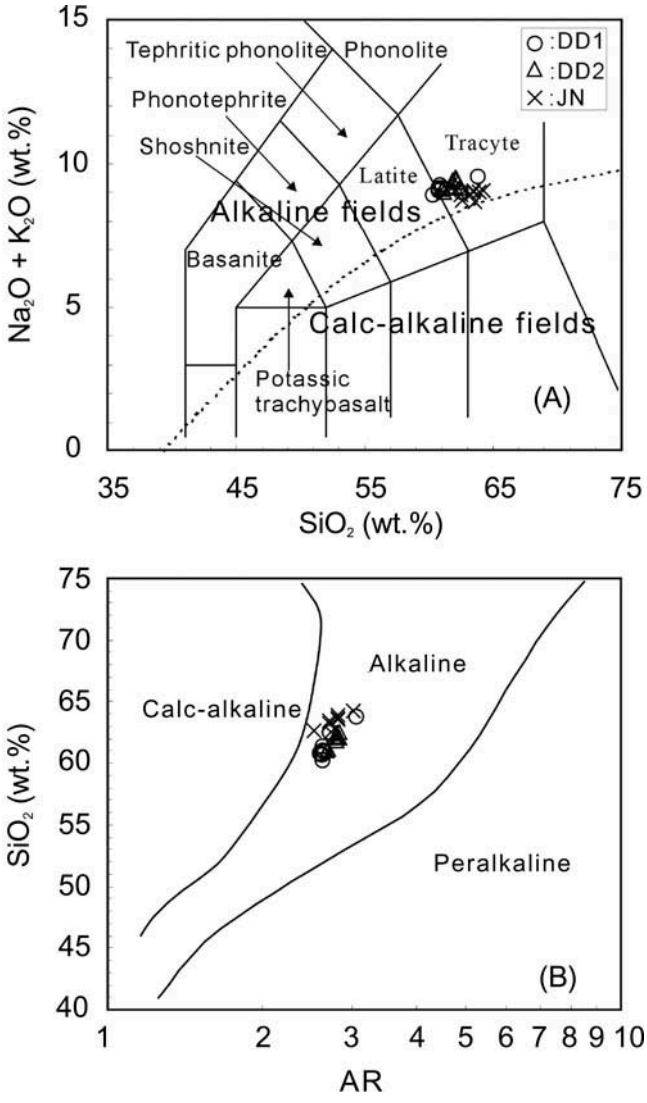

Figure 3. Classification of the adamellites from eastern Shandong Province on the basis of the total alkali–silica diagram (A); all of the major element data have been recalculated to 100% on a loss on ignition-free basis (after Middlemost 1994; Le Maitre 2002). SiO_2 *versus* AR (AR = $(Al_2O_3 + CaO + K_2O + Na_2O)/(Al_2O_3 + CaO–K_2O–Na_2O)$) showing the adamellites to be alkaline (after Wright 1969) (B).

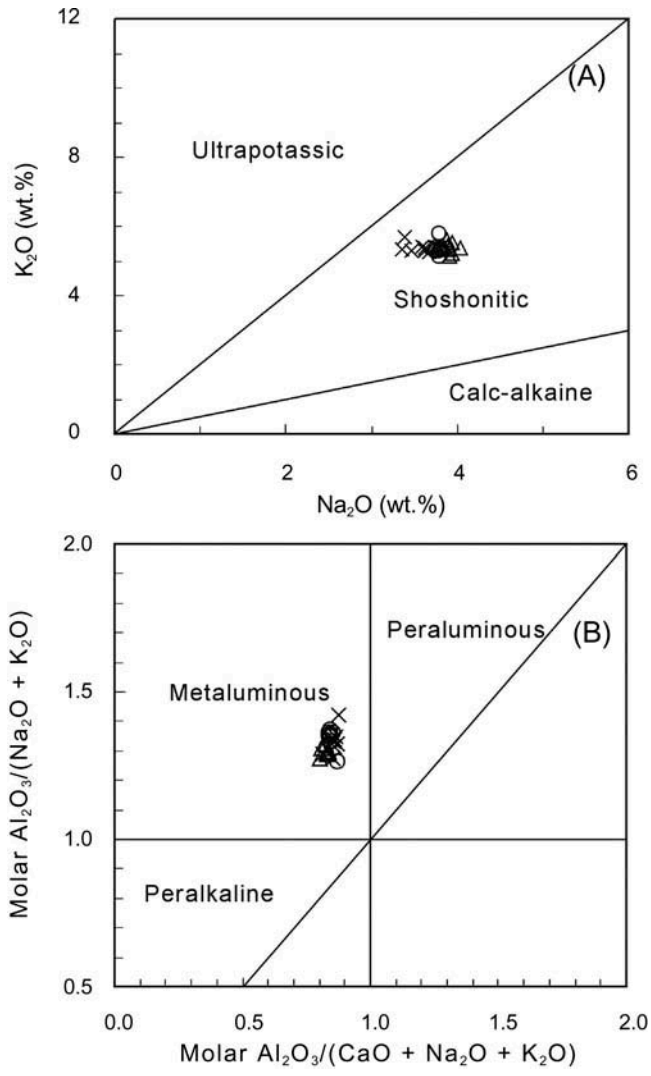

Figure 4. (A) K_2O *versus* Na_2O diagram showing the alkaline association to be shoshonitic (after Middlemost 1972). (B) molar $Al_2O_3/(Na_2O+K_2O)$ *versus* molar $Al_2O_3/(CaO + Na_2O + K_2O)$ plot, all samples fall in the metaluminous field.

patterns of the rocks show light rare earth element (LREE) enrichment and heavy rare earth element (HREE) depletion, with steep slopes (La_N/Yb_N = 15.0–46.0), small or moderate negative Eu anomalies (δEu = 0.46–0.75), and small positive Ce anomalies (δCe = 1.00–1.09) (Figure 8A). In addition, the adamellites are characterized by enrichment in large ion lithophile elements (LILEs, i.e. Rb, Th, Pb, and U) and depletion in Sr, Ba, and high field-strength elements (HFSEs, i.e. Nb, Ta, P, and Ti) (Figure 8B).

4.3. *Nd, Sr, and Pb isotopes*

Nine whole-rock Nd, Sr, and Pb isotopic data have been obtained from representative adamellite samples (Table 4). The rock samples show very uniform initial $^{87}Sr/^{86}Sr$ values from 0.7081 to 0.7089 $(^{87}Sr/^{86}Sr)_i$ and relatively small variation in strongly negative initial $\varepsilon_{Nd}(t)$ values from –16.70 to –17.80. The data are displayed in a figure (Figure 9) of $\varepsilon_{Nd}(t)$ *versus* $(^{87}Sr/^{86}Sr)_i$ ratios and are compared on that diagram with published compositional fields for late Mesozoic magmatic rocks from Shandong Province (Zhao *et al.* 1997; Fan *et al.* 2001), granites, mafic dikes, lamprophyres, syenites, and adakites (Yang 2000; Guo *et al*. 2004; Yang *et al*. 2005a, 2005b; Guo *et al*. 2006; Liu *et al*. 2008, 2010, 2012). Also shown are compositional trends from available data for components of the lower

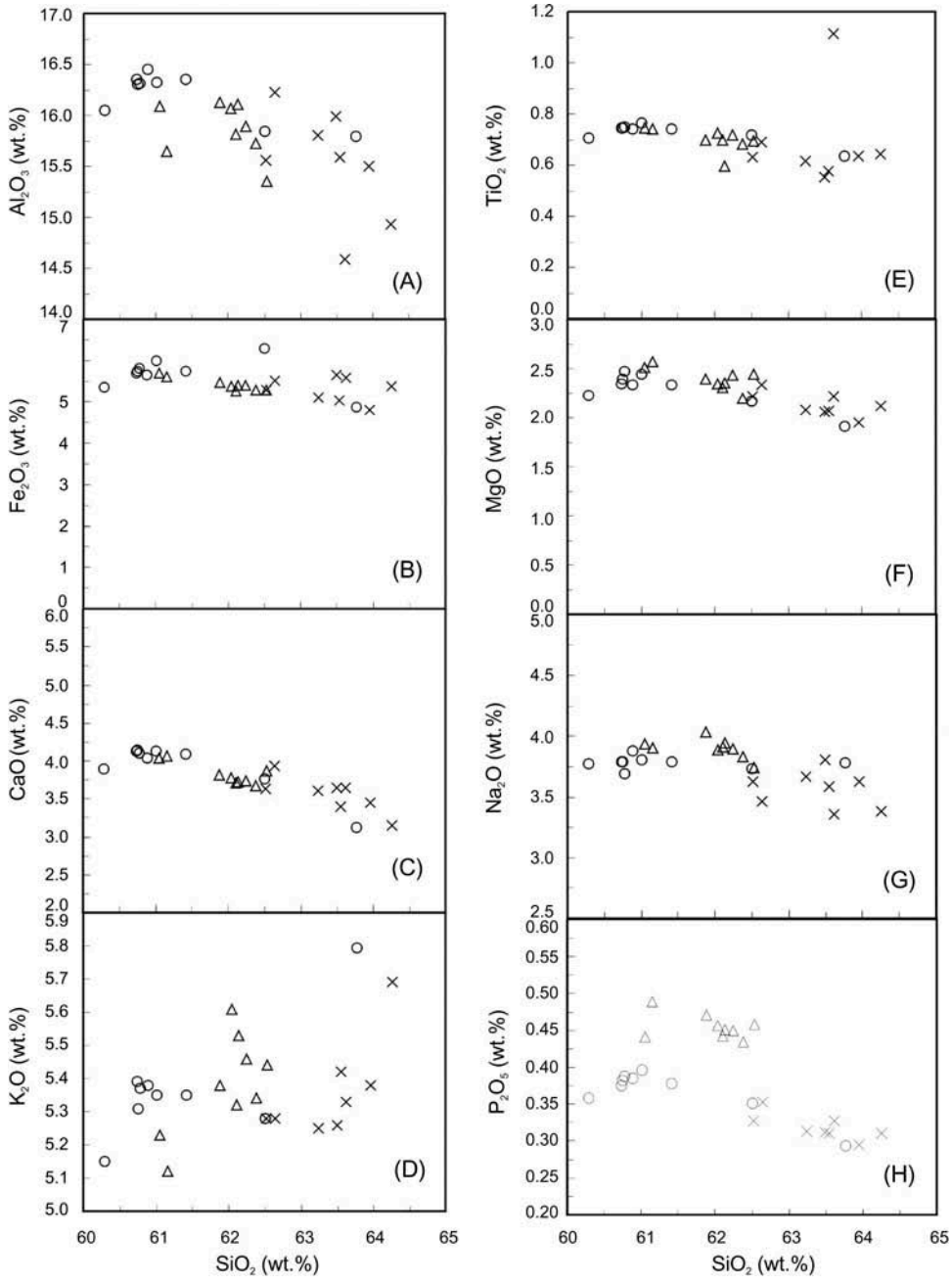

Figure 5. Whole-rock SiO_2 *versus* selected variation major element oxides diagrams for the adamellites from eastern Shandong Province.

and upper crust in the Jiaodong Peninsula from Shandong Province (Jahn *et al*. 1999). All of these rocks plot near the field of Early Cretaceous mafic volcanic rocks and syenites but far from those of lower and upper crust, Early Cretaceous granites, and mafic dikes (Figure 9). The model age (T_{DM}, depleted mantle age, Sm–Nd) of the adamellite samples is mainly in the range of 2.17–1.77 thousand million years. Previous geochemical studies of deeply derived xenoliths and mantle-derived magma from the NCC clearly demonstrated that the lithospheric mantle is enriched from the Palaeozoic to Mesozoic (Wang *et al*. 1996; Zhou *et al*. 2001). Consequently, the Nd isotopic model ages are considered to record the enrichment time of the NCC lithosphere mantle.

The adamellite Pb isotopic ratios are distinguished by $^{206}Pb/^{204}Pb = 16.938–17.149$, $^{207}Pb/^{204}Pb = 15.315–15.521$, and $^{208}Pb/^{204}Pb = 37.727–38.111$. These data are identical to those of basic igneous rocks and the Jiazishan alkaline complex from the central NCC (Zhang *et al*. 2004; Xie *et al*. 2006) and differ from those of the Yangtze lithospheric mantle (Yan *et al*. 2003), having a clear EM 1 tendency (Figure 10).

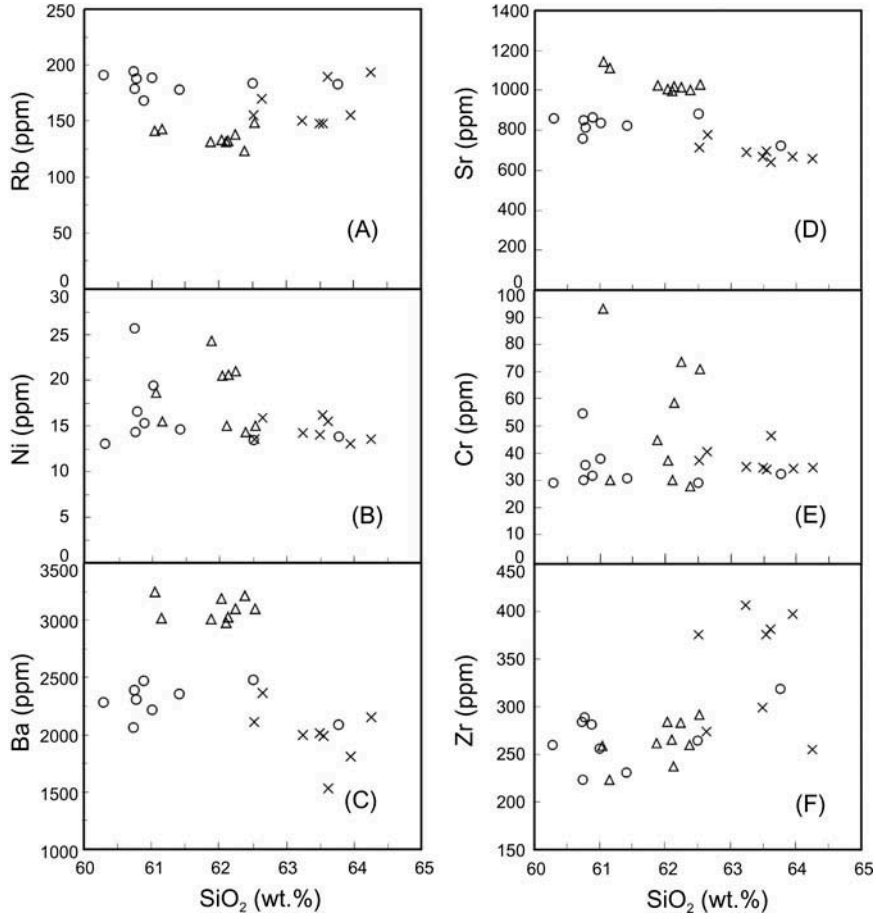

Figure 6. Whole-rock SiO_2 *versus* Rb, Ni, Ba, Sr, Cr, and Zr diagrams for the adamellites from eastern Shandong Province.

5. Petrogenetic discussion

5.1. *Source regions*

The negative initial $\varepsilon_{Nd}(t)$ values range from –16.70 to –17.80 (Table 4) for the adamellite samples and demonstrated that these rocks derived from the partial melting of an enriched lithospheric mantle rather than asthenospheric mantle, such as mid-ocean ridge basalt (MORB). An enriched lithospheric mantle is also confirmed by the Nd isotopic model ages (T_{DM}, 1.77–1.87 thousand million years, only one of 2.17 thousand million years). Previous studies in the region have revealed that the Yanshannian magmatic rocks in the Dabie–Sulu orogenic belt were similarly derived from an enriched lithosphere mantle. Nd isotopic model ages (T_{DM}) ranging from 1.4 to 2.0 thousand million years were acquired from these areas, which are consistent with those of the studied adamellites from eastern Shandong Province (Fan *et al*. 2001; Guo *et al*. 2001; Zhou *et al*. 2001). In addition, the studied adamellites possess high $(^{87}Sr/^{86}Sr)_i$ (0.7081–0.7089) and low $\varepsilon_{Nd}(t)$ values (–16.70 to –17.80) (Table 3), implying that these rocks originated from a lithospheric mantle rather than an asthenospheric mantle source, with a depleted Sr–Nd isotopic composition like that of MORB. A lithospheric mantle of NCC is further supported by the figure (Figure 9) of $\varepsilon_{Nd}(t)$ *versus* $(^{87}Sr/^{86}Sr)_i$ ratios of these rocks. In Figure 9, the adamellites have Sr–Nd isotopic features overlapping with the contemporaneous Rushan gabbros and associated mafic dikes (Meng *et al*. 2005) in Shandong Province, demonstrating their derivation from basaltic magma similar to the parental magmas of the mafic dikes. The adamellites share Pb isotopic characteristics (Table 3) different from those of the Yangtze Craton lithospheric mantle (Yan *et al*. 2003; Figure 10), which rules out involvement of Yangtze Craton lithosphere. In summary, the parental magma of the adamellites in the present study is derived from the melting of NCC lithospheric mantle.

5.2. *Fractional crystallization*

The low $Mg^{\#}$ (34.06–45.83), Cr (27.8–93.2 ppm), and Ni (13.1–25.7 ppm) of the adamellites is consistent with significant fractionation. For the studied adamellites,

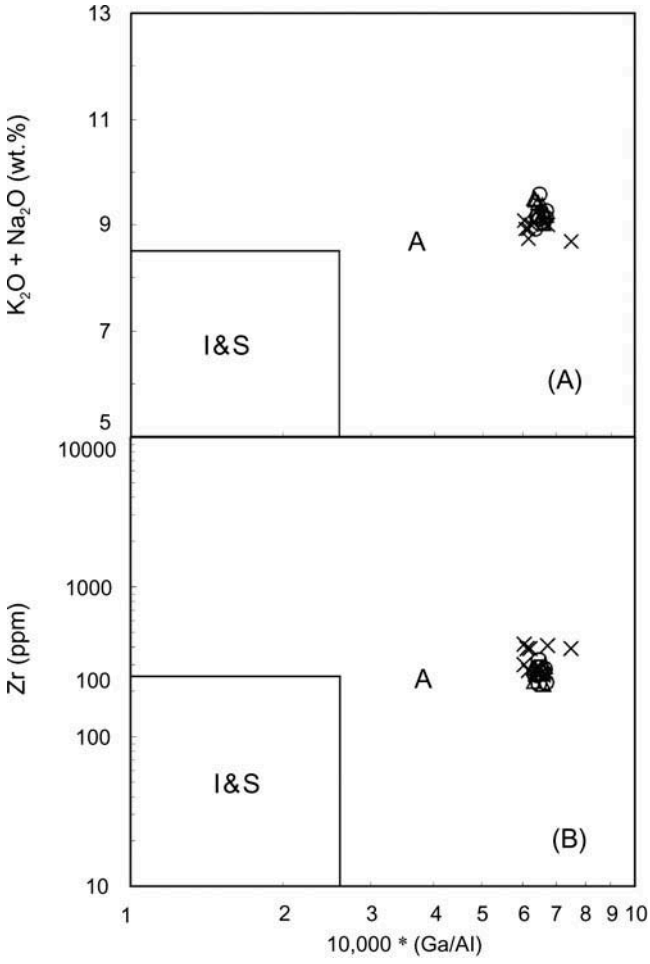

Figure 7. Plots of the adamellites in Zr and $K_2O + Na_2O$ *versus* 10,000 * (Ga/Al) diagrams of Whalen *et al.* (1987) showing affinity of A-type granites.

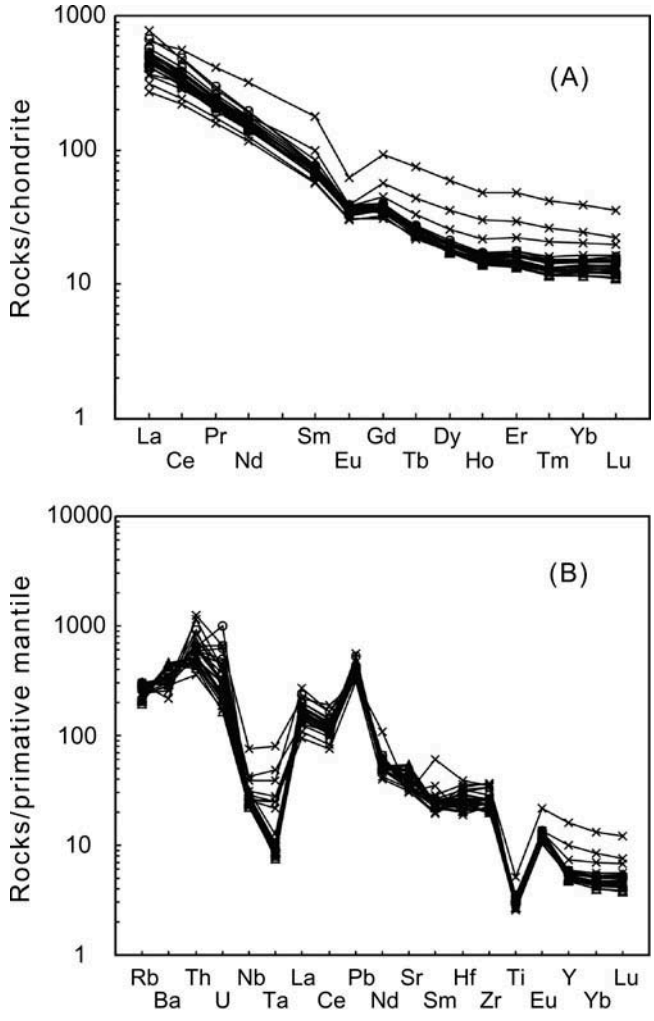

Figure 8. Whole-rock (A) chondrite-normalized rare earth element patterns and (B) primitive mantle-normalized spider diagrams of the adamellites from eastern Shandong Province. Chondrite and primitive mantle abundances are from Sun and McDonough (1989).

Al_2O_3 and CaO show a negative correlation with SiO_2 (Figures 5A and 5C), which is probably related to the fractionation of plagioclase. The negative correlation between MgO and SiO_2 indicates the fractionation and/or accumulation of clinopyroxene. Plagioclase and potassium feldspar fractional crystallization are supported by the relatively negative Ba, Sr, and Eu observed in the studied adamellites (Figure 8B). In addition, the presence of negative P and Ti anomalies in the analysed samples (Figure 8B) supports the fractionation of apatite and Ti-bearing oxides, such as rutile, ilmenite, and titanite.

5.3. *Crustal contamination*

Geochemical characteristics suggest that crustal contamination may have affected the petrogenesis of the eastern Shandong Province adamellites. These characteristics include the significant enrichment in Ba and LREE, and depletion in HFSE (Nb, Ta, and Ti). Crustal materials of NCC were involved in magma ascent by crustal contamination or in the source region duo to metasomatism. Jahn *et al*. (1999) suggested that the $\varepsilon_{Nd}(t)$ for the ancient lower crust is very low (–44 to –32), which is considerably lower than that for the adamellite samples (–17.80 to –16.70). Assimilation, crystal fractionation (AFC) and magma mixing would result in positive correlation between Nd and $\varepsilon_{Nd}(t)$ values. However, the lack of correlation between the $\varepsilon_{Nd}(t)$ values and Nd concentrations for the adamellites (Figure 11) indicate that magmatic evolution of the NCC adamellites in eastern Shandong Province was not significantly affected by crustal contamination and fractional crystallization as a major process during the late evolutionary stages. Therefore, the geochemical and isotopic signatures were mainly inherited from an enriched mantle source.

Table 3. Trace element contents (ppm) of the representative adamellites from eastern Shandong Province.

Sample	DD1-1	DD1-2	DD1-3	DD1-4	DD1-5	DD1-6	DD1-7	DD1-8	DD1-9	DD2-1	DD2-2	DD2-3	DD2-4	DD2-5	DD2-6	DD2-7	DD2-8	DD2-9	JN-1	JN-2	JN-3	JN-4	JN-5	JN-6	JN-7	JN-8	GBPG-1 RV*	GBPG-1 MV*	OU-6 RV*	OU-7 MV*
V	108	99.2	84.5	107	107	110	107	106	101	95.2	102	107	100	101	110	97.3	99.5	102	80.2	90.3	87.5	94.6	102	77.6	85.1	100	96.5	103	129	131
Cr	29.1	30.7	32.4	31.9	29.9	37.9	35.6	29.0	54.4	27.8	71.0	30.1	44.8	37.2	93.2	29.9	58.6	73.7	34.1	37.2	34.8	34.8	46.3	34.6	34.2	40.6	181	187	70.8	73.5
Ni	13.1	14.6	13.8	15.3	14.3	19.4	16.5	13.4	25.7	14.3	15.0	15.5	24.3	20.5	18.6	15.0	20.6	21.0	16.2	13.6	14.2	13.5	15.5	14.0	13.1	15.9	59.6	60.6	39.8	42.5
Ga	26.9	29.0	27.1	29.0	27.9	27.7	28.2	27.6	27.9	26.6	27.1	27.4	27.5	26.9	27.7	27.5	27.1	27.5	25.7	25.3	25.4	26.1	28.9	25.6	27.6	26.5	18.6	20.9	24.3	26.5
Rb	191	178	183	168	179	189	188	184	194	124	148	143	131	133	142	132	132	138	148	155	150	194	189	148	155	170	56.2	61.4	120	122
Sr	862	825	721	863	850	838	814	881	759	1004	1031	1110	1026	1008	1146	996	1021	1016	697	714	693	660	642	667	667	777	364	377	131	136
Ba	2286	2359	2084	2470	2386	2218	2310	2480	2065	3214	3096	3014	3007	3187	3245	2981	3030	3103	1985	2114	2000	2148	1529	2013	1808	2363	18.6	20.9	477	486
Zr	262	231	324	284	224	258	292	266	288	262	295	223	264	287	261	267	238	287	383	384	416	257	389	303	406	277	0.40	0.50	174	183
Hf	8.05	7.26	10.0	8.36	7.29	7.80	8.86	8.22	9.02	7.00	8.17	6.87	7.23	7.91	7.89	7.15	6.41	7.75	9.81	9.44	10.5	5.78	11.9	8.05	11.2	6.17	232	224	4.70	4.90
Nb	18.3	19.2	20.4	19.2	18.1	19.3	19.0	18.5	22.0	17.9	17.9	16.7	18.6	18.4	16.8	17.4	15.9	19.9	18.8	22.0	20.3	30.1	53.7	18.2	27.8	18.5	908	921	14.8	15.3
Ta	0.37	0.37	0.44	0.39	0.38	0.37	0.37	0.37	0.51	0.41	0.37	0.35	0.39	0.35	0.35	0.31	0.33	0.41	1.03	1.16	1.04	2.02	3.33	1.02	1.61	0.90	14.1	14.5	1.10	1.00
U	6.82	13.1	5.69	7.67	10.4	13.9	20.9	9.28	8.77	5.08	6.44	5.00	3.99	4.52	5.41	4.56	3.48	4.35	4.58	6.33	5.14	8.30	13.8	3.69	8.50	6.43	0.90	0.99	1.96	2.19
Th	55.2	50.8	77.4	52.4	50.4	55.8	53.8	48.6	60.6	43.7	42.1	40.4	37.3	37.1	37.7	38.1	35.4	39.0	46.8	51.1	46.0	96.5	105	30.5	72.0	40.7	11.5	13.9	11.2	11.4
Pb	25.9	25.6	28.4	31.2	38.0	28.3	28.7	29.6	28.2	33.4	27.7	24.6	24.2	25.2	26.9	23.6	24.6	24.8	39.7	24.7	25.8	25.6	22.1	21.9	23.2	24.7	11.2	11.4	28.2	32.7
Sc	12.1	12.3	11.5	12.3	12.2	13.4	12.4	12.2	11.8	10.8	13.1	11.9	13.6	12.2	13.7	11.2	11.3	14.2	11.7	12.5	10.9	13.5	11.9	10.3	10.3	11.2	13.9	14.2	22.1	21.6
Y	25.9	25.4	24.4	25.9	25.1	27.1	26.0	25.7	25.9	22.3	22.0	22.6	23.3	23.0	22.5	21.7	21.5	23.9	23.8	26.9	24.6	45.8	73.5	23.7	33.7	23.3	18.0	17.2	27.4	26.2
La	137	114	161	116	114	137	127	120	121	110	104	98.3	112	107	110	126	100	112	74.0	85.7	97.0	87.2	151	64.3	184	104	103	105	33.0	33.1
Ce	253	208	295	211	215	250	237	231	222	195	199	192	204	199	205	213	183	207	147	172	184	195	340	133	289	197	11.5	11.6	74.4	78.0
Pr	24.7	21.5	28.2	21.6	21.5	24.7	23.4	22.7	22.4	19.8	20.2	19.7	20.8	20.5	20.7	21.5	18.7	21.2	16.4	19.2	19.4	22.3	38.8	15.1	26.8	19.5	43.3	42.4	7.80	8.10
Nd	82.5	73.0	90.5	73.9	74.3	82.5	78.9	77.5	75.0	67.4	69.5	68.4	71.4	71.2	71.4	72.9	65.3	72.7	58.1	67.3	66.1	83.2	147.9	54.3	88.1	66.9	6.80	6.60	29.0	30.6
Sm	11.7	10.8	11.9	11.0	11.1	11.9	11.4	11.4	10.9	9.94	10.3	10.4	10.7	10.7	10.7	10.5	9.87	10.8	8.89	10.4	9.80	15.3	26.9	8.62	12.8	9.76	1.79	1.69	5.92	5.99
Eu	2.26	2.09	2.04	2.00	2.13	2.20	2.18	2.21	1.89	2.15	2.09	2.20	2.10	2.06	2.17	2.10	2.10	2.26	1.79	1.92	2.02	2.28	3.61	1.73	2.22	1.98	4.74	4.47	1.36	1.35
Gd	8.22	7.62	7.81	7.51	7.67	8.01	8.18	8.20	7.25	7.06	7.12	7.49	7.29	7.60	7.59	7.28	6.96	7.60	6.40	7.50	7.41	11.65	19.13	6.70	9.15	7.60	0.60	0.59	5.27	5.50
Tb	1.01	0.96	0.99	0.96	0.97	1.02	1.00	1.00	0.95	0.84	0.91	0.90	0.92	0.90	0.94	0.91	0.87	0.96	0.86	0.99	0.91	1.62	2.79	0.81	1.23	0.90	3.26	3.17	0.85	0.83
Dy	5.20	4.95	4.90	5.05	5.00	5.40	5.18	5.14	4.90	4.34	4.33	4.60	4.73	4.62	4.55	4.47	4.37	4.92	4.56	5.13	4.91	8.98	15.2	4.51	6.57	4.61	0.69	0.66	5.0	5.06
Ho	0.95	0.92	0.88	0.94	0.93	0.98	0.96	0.97	0.91	0.83	0.80	0.84	0.85	0.83	0.84	0.79	0.79	0.87	0.87	0.96	0.90	1.73	2.76	0.87	1.22	0.87	2.01	2.02	1.0	1.02
Er	2.75	2.68	2.69	2.69	2.65	2.90	2.76	2.80	2.68	2.39	2.27	2.34	2.46	2.41	2.32	2.28	2.23	2.54	2.66	2.90	2.66	4.85	7.93	2.50	3.71	2.46	0.30	0.29	2.98	3.07
Tm	0.39	0.37	0.36	0.38	0.38	0.39	0.39	0.38	0.39	0.32	0.30	0.32	0.33	0.32	0.32	0.30	0.30	0.34	0.39	0.41	0.37	0.67	1.07	0.34	0.52	0.33	2.03	2.03	0.44	0.45
Yb	2.55	2.49	2.51	2.51	2.55	2.60	2.57	2.58	2.64	2.20	2.09	2.09	2.19	2.13	2.07	1.98	1.97	2.27	2.59	2.79	2.58	4.18	6.59	2.35	3.48	2.30	0.31	0.31	3.00	3.09
Lu	0.39	0.37	0.39	0.37	0.37	0.39	0.38	0.38	0.41	0.33	0.32	0.30	0.33	0.32	0.31	0.28	0.29	0.34	0.37	0.42	0.39	0.56	0.90	0.35	0.50	0.36	6.07	5.93	0.45	0.47
Σ REE	533	450	609	456	458	529	500	486	474	423	423	410	440	429	438	464	397	446	324	378	399	439	765	296	629	419				
$(La/Yb)_N$	38.5	32.8	46.0	33.3	31.9	37.6	35.3	33.3	33.0	35.8	35.7	33.7	36.8	36.0	38.0	45.6	36.4	35.5	20.5	22.1	27.0	15.0	16.4	19.7	38.0	32.6				
SEu	0.67	0.67	0.61	0.64	0.67	0.65	0.66	0.67	0.61	0.75	0.71	0.73	0.69	0.67	0.70	0.70	0.74	0.73	0.69	0.64	0.70	0.50	0.46	0.67	0.60	0.68				

Notes: RV*, recommended values; MV*, measured values. Values for GBPG-1 are from Thompson *et al.* (2000); values for OU-6 are from Potts and Kane (2005).

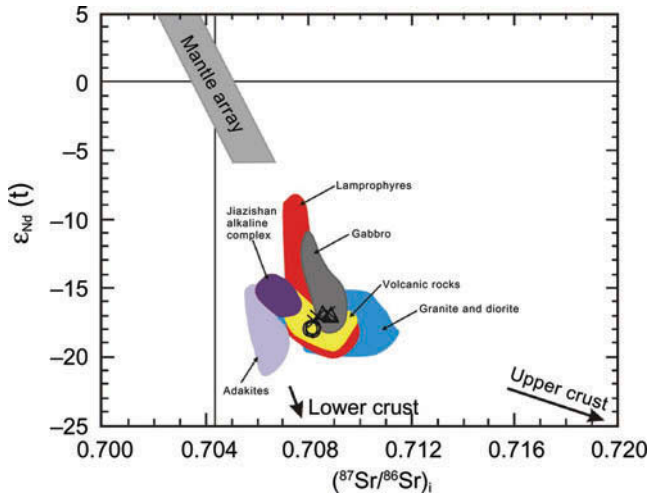

Figure 9. Initial $^{87}Sr/^{86}Sr$ *versus* $\varepsilon_{Nd}(t)$ diagram for the adamellites from Shandong Province. The illustrated data field for Jiazishan alkaline complex is from Yang *et al.* (2005a, 2005b), lamprophyres are from Guo *et al.* (2004), gabbro is from Meng *et al.* (2005), volcanic rocks are from Fan *et al.* (2001), granite and diorite are from Huang *et al.* (2005), and adakites are from Guo *et al.* (2006).

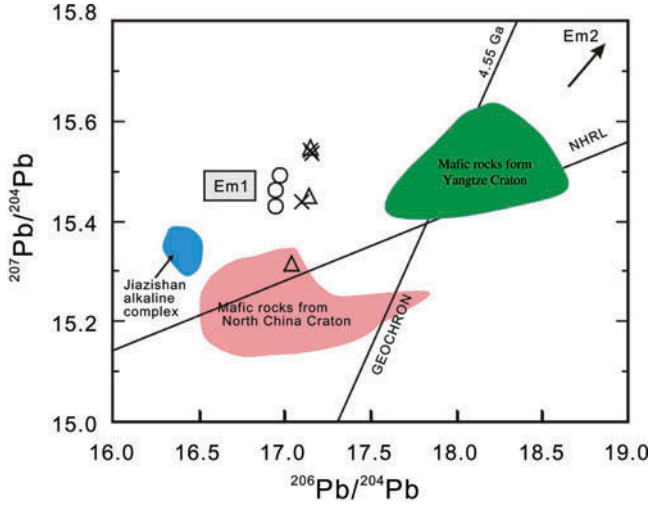

Figure 10. $^{207}Pb/^{204}Pb$ *versus* $^{206}Pb/^{204}Pb$ diagrams for the adamellites, compared with those of Early Cretaceous mafic rocks from the North China and Yangtze cratons. Northern hemisphere regression line (NHRL) and 4.55 Ga geochron are from Zou *et al*. (2000) and Hart (1984), respectively. Mafic rock data of North China Craton are from Zhang *et al*. (2004) and Xie *et al*. (2006) and of Yangtze Craton are from Yan *et al*. (2003).

5.4. Petrogenetic model

At present, there are three petrogenetic models for alkaline felsic rocks. First, the alkaline felsic magma may be products of fractionation of mantle-derived magma with or without crustal contamination (Zhong *et al*. 2007 and references therein). Second, the alkaline felsic magma may have originated by partial melting of lower-crustal rocks under fluxing of volatiles (Lubala *et al*. 1994).

Table 4. Sr–Nd–Pb isotopic composition of the representative adamellites from eastern Shandong Province.

Sample	Age (Ma)	Sm (ppm)	Nd (ppm)	Rb (ppm)	Sr (ppm)	$^{147}Sm/^{144}Nd$	$^{143}Nd/^{144}Nd$	2σ	$(^{143}Nd/^{144}Nd)_i$	$\varepsilon_{Nd}(t)$	$f_{Sm/Nd}$	T_{DM} (Ma)	$^{87}Rb/^{86}Sr$	$^{87}Sr/^{86}Sr$	2σ	$(^{87}Sr/^{86}Sr)_i$	$^{206}Pb/^{204}Pb$	$^{207}Pb/^{204}Pb$	$^{208}Pb/^{204}Pb$
DD1-4	122.1	11.38	78.96	188	813	0.087	0.511638	9	0.511568	−17.80	−0.558	1817	0.573	0.70914	9	0.70815	16.938	15.445	37.882
DD1-5	122.1	11.12	74.21	178	851	0.091	0.511647	8	0.511574	−17.69	−0.537	1864	0.520	0.70915	12	0.70825	16.966	15.470	37.933
DD1-7	122.1	10.73	73.54	169	864	0.088	0.511639	11	0.511569	−17.80	−0.553	1830	0.486	0.70901	16	0.70817	16.938	15.416	37.727
DD2-4	122.1	10.10	65.40	133	1023	0.093	0.511695	10	0.511621	−16.78	−0.527	1835	0.323	0.70944	14	0.70888	17.143	15.521	38.111
DD2-5	122.1	10.66	71.98	133	1008	0.090	0.511694	12	0.511622	−16.76	−0.542	1792	0.326	0.70914	13	0.70858	17.139	15.435	37.846
DD2-8	122.1	11.07	71.60	131	1025	0.093	0.511696	8	0.511622	−16.76	−0.527	1834	0.317	0.70940	10	0.70885	17.032	15.315	37.744
JN-1	123.2	9.72	66.74	169	776	0.088	0.511685	9	0.511614	−16.89	−0.553	1774	0.541	0.70931	12	0.70836	17.092	15.424	37.701
JN-6	123.2	8.67	54.50	147	666	0.096	0.511702	8	0.511625	−16.68	−0.512	1872	0.548	0.70973	11	0.70877	17.142	15.515	38.061
JN-8	123.2	15.32	83.80	192	659	0.111	0.511682	11	0.511593	−17.31	−0.436	2174	0.723	0.70955	12	0.70828	17.149	15.511	38.043

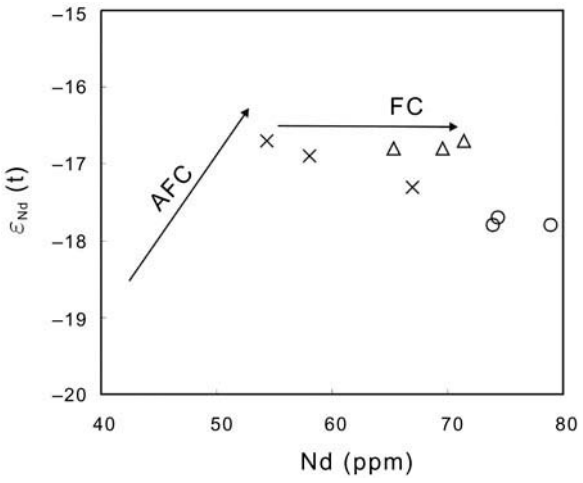

Figure 11. Whole-rock $\varepsilon_{Nd}(t)$ *versus* Nd for the adamellites from eastern Shandong Province.

Third, the alkaline felsic magma may result from mixing of basic and silicic melts and their differentiates (Sheppard 1995; Litvinovsky *et al*. 2002).

Several extensive studies on the Mesozoic alkaline complex in Shandong Province have been conducted. For example, Gao *et al*. (2008) previously studied the granitoids, which could be derived from dehydration melting of the lower crust due to underplating of mantle-derived basaltic magma. However, it is unlikely that the extensive melting of the lower crust can occur when basaltic melts underplate the lower crust (Defant *et al*. 2002). Based on our data and their explanation, the probability of crustal assimilation has already been ruled out. Therefore, the involvement of crustal components in the source is suggested. Therefore, we prefer fractionation of mantle-derived magma without crustal contamination as the most probable model for the origin of the adamellites.

A scenario for the origin of the adamellites in eastern Shandong Province or the Sulu Belt is presented. At 205–185 Ma, intra-continental compression between the NCC and Yangtze Block possibly thickened the crust and induced eclogitization of the thickened lower crust. Given the higher density of eclogite than that of lithospheric mantle peridotite of 0.2–0.4 g cm^{-3} (Jull and Kelemen 2001; Anderson 2006; Levander *et al.* 2006), eclogite can be recycled into the mantle (Kay and Kay 1991; Jull and Kelemen 2001; Gao *et al.* 2004). During 185–165 Ma, lithospheric delamination, mainly foundering of eclogite from the lower thickened crust, occurred beneath the Dabie–Sulu orogenic belt (Li *et al.* 2002), triggering asthenospheric upwelling, sudden uplift of the Sulu Belt, and orogenic collapse as well as lithospheric extension and thinning. On the other hand, these rocks have lower melting temperatures than mantle peridotite (Rapp *et al.* 1999; Kogiso *et al.* 2003; Sobolev *et al.* 2005, 2007) and, as foundered silica-saturated eclogite heats up, eclogite will produce silicic melts (tonalite to trondhjemite) that may hybridize variably with overlying mantle peridotite. Between 130 and 110 Ma (Li *et al.* 2002), decompressional melting of the metasomatized lithospheric mantle produced primary magma in the form of basaltic melts. Subsequently, magma ascent and fractionation occurred resulting in the emplacement of the adamellites across the NCC.

6. Conclusions

Based on our new geochronological, geochemical, and Sr–Nd–Pb isotopic data, we draw the following conclusions concerning the origins of the adamellites.

(1) The U–Pb zircon age data indicate that the studied adamellites crystallized at 120.3 ± 2.1 to 123.2 ± 1.8 Ma. The adamellites show shoshonitic whole-rock affinities based on their K_2O and Na_2O contents. The rocks have high LREEs [$(La/Yb)_N$ = 15.0–46.0], show negative Eu anomalies (δEu = 0.46–0.75), positive Rb, Th, Pb, and U anomalies, and are depleted in Sr, Ba, and HFSEs (i.e. Nb, Ta, P, and Ti). The studied rocks all show relatively low radiogenic Sr [$(^{87}Sr/^{86}Sr)_i = 0.7081–0.7089$], negative initial $\varepsilon_{Nd}(t)$ values from –16.7 to –17.8, and Pb isotopic ratios ($^{206}Pb/^{204}Pb$ = 16.882–17.149, $^{207}Pb/^{204}Pb$ = 15.315–15.521, $^{208}Pb/^{204}Pb$ = 37.544–38.111), suggesting origination from low-degree partial melting of an enriched mantle below the NCC.

(2) The parent magma probably originated via fractional crystallization of potassium feldspar, plagioclase and Fe–Ti oxides (e.g. rutile, ilmenite, and titanite), apatite, and zircon during the ascent of alkaline rocks without crustal contamination. Zircon saturation temperatures (T_{Zr}) of the adamellites are 830–903°C, approximately representing the crystallization temperature of the alkaline magma. Intense lithospheric thinning beneath the Sulu Belt of eastern China that occurred at ~120 Ma was caused by foundering of the lower lithosphere (mantle and lower crust).

Acknowledgements

This research was supported by the National Nature Science Foundation of China (41103017) and State Key Laboratory of Ore Deposit Geochemistry Open Foundation of the Institute of Geochemistry, Chinese Academy of Sciences (201105). We are grateful to Guixiang Yu for assisting in the analysis of the Sr, Nd, and Pb isotopes and to Hangqiang Xie for assisting with the SHRIMP zircon U–Pb dating. Thanks are also due to Shandong Province Experimental Institute of Geological Sciences.

References

Anderson, D.A., 2006, Speculations on the nature and cause of mantle heterogeneity: Tectonophysics, v. 146, p. 7–22.

Black, L.P., Kamo, S.L., Allen, C.M., Aleinikoff, J.N., Davis, D.W., Korsch, R.J., and Foudoulis, C., 2003, TEMORA 1: A new zircon standard for Phanerozoic U-Pb geochronology: Chemical Geology, v. 200, p. 155–170.

Bonin, B., Platevoet, B., and Vialette, Y., 1987, The geodynamic significance of alkaline magmatism in the Western Mediterranean compared with West Africa: Geological Journal, v. 22, p. 361–387.

Chavagnac, V., and Jahn, B.-M., 1996, Coesite-bearing eclogites from the Bixiling complex, Dabie Mountains, China: Sm-Nd ages, geochemical characteristics and tectonics implications: Chemical Geology, v. 133, p. 29–51.

Chen, J.F., Xie, Z., Li, H.M., Zhang, X.D., Zhou, T.X., Park, Y.S., Ahn, K.S., Chen, D.G., and Zhang, H., 2003, U-Pb zircon ages for a collision-related K-rich complex at Shidao in the Sulu ultrahigh pressure terrane, China: Chemical Geology, v. 37, p. 35–46.

Compston, W., Williams, I.S., Kirschvink, J.L., Zhang, Z., and Ma, G., 1992, Zircon U-Pb ages for the Early Cambrian timescale: Journal of Geology Society, v. 149, p. 1481–71.

Cong, B.L., 1996, Ultrahigh-pressure metamporphic rocks in the Dabie-Sulu region of China: Beijing, China, Science Press and Dordrecht, Kluwer Academic Publishing, p. 224.

Defant, M.J., Kepezhinskas, P., Defant, M.J., Xu, J.F., Kepezhinskas, P., Wang, Q., Zhang, Q., and Xiao, L., 2002, Adakites: Some variations on a theme: Acta Petrologica Sinica, v. 18, p. 129–142.

Enami, M., and Zang, Q., 1993, High-pressure eclogite from northern Jiangsu and southern Shandong province, eastern China: Journal of Metamorphic Geology, v. 11, p. 589–603.

Fan, W.M., Guo, F., Wang, Y.J., Lin, G., and Zhang, M., 2001, Postorogenic bimodal volcanism along the Sulu orogenic belt in eastern China: Physics and Chemistry of the Earth, Part A Solid Earth Geology, v. 26, p. 733–746.

Gao, S., Rudnick, R.L., Xu, W.L., Yuan, H.L., Liu, Y.S., Walker, R.J., Puchtel, I., Liu, X.M., Huang, H., Wang, X.R., and Yang, J., 2008, Recycling deep cratonic lithosphere and generation of intraplate magmatism in the North China Craton: Earth and Planetary Science Letters, v. 270, p. 41–53.

Gao, S., Rudnick, R.L., Yuan, H.L., Liu, X.M., Liu, Y.S., Xu, W.L., Ling, W.L., Ayers, J., Wang, X.C., and Wang, Q.H., 2004, Recycling lower continental crust in the North China Craton: Nature, v. 432, p. 892–897.

Guo, F., Fan, W.M., and Li, C.M., 2006, Geochemistry of late Mesozoic adakites from the Sulu belt, eastern China: Magma genesis and implications for crustal recycling beneath continental collisional orogens: Geological Magazine, v. 143, p. 1–13.

Guo, F., Fan, W.M., Wang, Y.J., and Lin, G., 2001, Late Mesozoic mafic intrusive complexes in North China Block: Constraints on the nature of subcontinental lithospheric mantle: Physics and Chemistry of the Earth (A), v. 26, p. 759–771.

Guo, F., Fan, W.M., Wang, Y.J., and Zhang, M., 2004, Origin of Early Cretaceous calc-alkaline lamprophyres from the Sulu orogen in eastern China: Implications for enrichment processes beneath continental collisional belt: Lithos, v. 78, p. 291–305.

Guo, J.H., Chen, F.K., Zhang, X.M., Siebel, W., and Zhai, M.G., 2005, Evolution of syn- to post-collisional magmatism from north Sulu UHP belt, eastern China: Zircon U-Pb geochronology: Acta Petrologica Sinica, v. 21, p. 1281–1301.

Hacker, B., Ratschbacher, L., Webb, L., Ireland, T., Walker, D., and Dong, S., 1998, U/Pb zircon ages constrain the architecture of the ultrahigh-pressure Qinling-Dabie Orogen, China: Earth and Planetary Science Letters, v. 161, p. 215–230.

Hart, S.R., 1984, A large-scale isotope anomaly in the Southern Hemisphere mantle: Nature, v. 309, p. 753–757.

Hirajima, T., Ishiwatari, A., Cong, B., Zhang, R., Banno, S., and Nozaka, T., 1990, Coesite from Mengzhong eclogite at Donghai county, northern Jiangsu province, China: Mineralogical Magazine, v. 54, p. 579–583.

Hong, D.W., Wang, T., Tong, Y., and Wang, X.X., 2003, Mesozoic granitoids from North China Block and Qinling-Dabie-Sulu orogenic belt and their deep dynamic process: Earth Science Frontiers, v. 10, p. 231–256.

Huang, C., 1978, An outline of the tectonic characteristics of China: Eclogae Geologicae Helvetiae, v. 71, p. 611–635.

Huang, J., Zheng, Y.F., Wu, Y.B., and Zhao, Z.F., 2005, Geochemistry of elements and isotopes in igneous rocks from the Wulian region in the Sulu orogen: Acta Petrologica Sinica, v. 21, p. 545–568.

Jahn, B.M., Wu, F.Y., Lo, C.H., and Tsai, C.H., 1999, Crust mantle interaction induced by deep subduction of the continental crust: Geochemical and Sr-Nd isotopic evidence from post-collisional mafic-ultramafic intrusions of the northern Dabie complex, central China: Chemical Geology, v. 157, p. 119–146.

Jull, M., and Kelemen, P.B., 2001, On the conditions for lower crustal convective instability: Journal of Geophysical Research, v. 106, p. 6423–6446.

Kato, T., Enami, A., and Zhai, M., 1997, Ultrahigh-pressure marble and eclogite in the Su-Lu ultrahigh pressure Terrane, eastern China: Journal of Metamorphic Geology, v. 15, p. 169–182.

Kay, R.W., and Kay, S.M., 1991, Creation and destruction of lower continental crust: Geologische Rundschau, v. 80, p. 259–278.

Kogiso, T., Hirschmann, M.M., and Frost, D.J., 2003, High pressure partial melting of garnet pyroxenite: Possible mafic lithologies in the source of ocean island basalts: Earth and Planetary Science Letters, v. 216, p. 603–617.

Le Maitre, R.W., 2002, Igneous rocks: A classification and glossary of terms (second edition): Cambridge, Cambridge University Press, 236 p.

Levander, A., Niu, F., Lee, C.T.A., and Cheng, X., 2006, Imaging the continental lithosphere: Tectonophysics, v. 416, p. 167–185.

Li, S.G., Huang, F., and Li, H., 2002, Post-collisional delamination of the lithosphere beneath Dabie-Sulu orogenic belt: Chinese Science Bulletin, v. 46, p. 1487–1490.

Litvinovsky, B.A., Jahn, B.M., Zanvilevich, A.N., Shadaev, M.G., 2002, Crystal fractionation in the petrogenesis of an alkali monzodiorite-syenite series: The Oshurkovo plutonic sheeted complex, Transbaikalia, Russia: Lithos, v. 64, p. 97–130.

Liu, S., Hu, R.Z, Gao, S., Feng, C.X., Feng, G.Y., Coulson, I.M., Li, C., Wang, T., and Qi, Y.Q., 2010, Zircon U-Pb age and Sr-Nd-Hf isotope geochemistry of Permian granodiorite and associated gabbro in the Songliao Block, NE China and implications for growth of juvenile crust: Lithos, v. 114, p. 423–436.

Liu, S., Hu, R.Z., Gao, S., Feng, C.X., Feng, G,Y., Qi, Y.Q., Coulson, I.M., Yang, Y.H., Yang, C.G., and Tang, L., 2012, Geochemical and isotopic constraints on the age and origin of mafic dikes from eastern Shandong Province, eastern North China Craton: International Geology Review, v. 54, p. 1389–1400.

Liu, S., Hu, R.Z, Gao, S., Feng, C.X., Qi, L., Zhao, J.H., Zhong, H., Qi, Y.Q., and Wang, T., 2008, K-Ar ages, geochemical and Sr-Nd isotopic compositions of the Adakitic volcanic rocks in western Shandong Province: Evidence for foundering of lower continental crust: International Geology Review, v. 50, p. 763–779.

Liu, S., Hu, R.Z., Zhao, J.H., and Feng, C.X., 2004, K-Ar geochronology of Mesozoic mafic dikes in Shandong Province, eastern China: Implications for crustal extension: Acta Geologica Sinica, v. 78, p. 1207–1213.

Lubala, R.T., Frick, C., Roders, J.H., and Walraven, F., 1994, Petrogenesis of syenites and granites of the Schiel Alkaline complex, Northern Transvaal, South Africa: Journal Geology, v. 102, p. 307–309.

Meng, F.C., Xue, H.M., Li, T.F., Yang, H.R., and Liu, F.L., 2005, Enriched characteristics of Late Mesozoic mantle under the Sulu orogenic belt: Geochemical evidence from gabbro in Rushan: Acta Petrologica Sinica, v. 21, p. 1583–1592.

Middlemost, E.A.K., 1972, A simple classification of volcanic rocks: Bulletin of Volcanology, v. 36, p. 382–397.

Middlemost, E.A.K., 1994, Naming materials in the magma/igneous rock system: Earth-Science Reviews, v. 74, p. 193–227.

Miller, C., Schuster, R., Klötzli, U., Frank, W., and Purtscheller, F., 1999, Post-collisional potassic and ultrapotassic magmatism in SW Tibet: Geochemical and Sr-Nd-Pb-O isotopic constraints for mantle source characteristics and petrogenesis: Journal of Petrology, v. 40, p. 1399–1424.

Potts, P.J., and Kane, J.S., 2005, International association of geoanalysts certificate of analysis: Certified reference material OU-6 (Penrhyn slate): Geostandards and Geoanalytical Research, v. 29, p. 233–236.

Qi, L., Hu, J., and Grégoire, D.C., 2000, Determination of trace elements in granites by inductively coupled plasma mass spectrometry: Talanta, v. 51, p. 507–513.

Rapp, R.P., Shimizu, N., Norman, M.D., and Applegate, G.S., 1999, Reaction between slab-derived melts and peridotite in the mantle wedge: Experimental constraints at 3.8 GPa: Chemical Geology, v. 160, p. 335–356.

Ren, K.Y., 2003, Study progress of the alkaline rocks: A review: Geology of Chemical Minerals, v. 25, p. 151–163 (in Chinese with English abstract).

Sheppard, S., 1995, Hybridization of shoshonitic lamprophyre and calc-alkaline granite magma in the Early Proterozoic Mt. Bundey igneous suite, Northern Territory. Aust: Journal of Earth Science, v. 42, p. 173–185.

Sobolev, A.V., Hofmann, A.W., Kuzmin, D.V., Yaxley, G.M., Arndt, N.T., Chung, S.L., Danyushevsky, L.V., Elliott, T., Frey, F.A., and Garcia, M.O., 2007, The amount of recycled crust in sources of mantle-derived melts: Science, v. 316, p. 412–417.

Sobolev, A.V., Hofmann, A.W., Sobolev, S.V., and Nikogosian, I.K., 2005, An olivine-free mantle source of Hawaiian shield basalts: Nature, v. 434, p. 590–597.

Song, B., Zhang, Y.H., Wan, Y.S., and Jian, P., 2002, Mount Making and procedure of the SHRIMP dating. Geological Review, v. 48, p. 26–30. (Suppl., in Chinese).

Sun, S.S., and McDonough, W.F., 1989, Chemical and isotopic systematics of oceanic basalts: Implications for mantle composition and processes, *in* Saunders, A.D., and Norry, M.J., eds., Magmatism in the ocean basins: London, Geological Society Special Publication, p. 313–345.

Thompson, M., Potts, P.J., Kane, J.S., and Wilson, S., 2000, An international proficiency test for analytical geochemistry laboratories-report on round 5 (August 1999): Geostandards and Geoanalytical Research, v. 24, p. E1–E28.

Wang, D.Z., Ren, Q.J., Qiu, J.S., Chen, K.R., Xu, Z.W., and Zen, J.H., 1996, Characteristics of volcanic rocks in the shoshonite province, eastern China, and their metallogenesis: Acta Geologica Sinica, v. 70, p. 23–34.

Wang, L.G., Qiu, Q., McNaughton, N.J., Groves, D.I., Luo, Z., Huang, J., Miao, L., and Liu, Y., 1998, Constraints on crustal evolution and gold metallogeny in the Northwestern Jiaodong Peninsula, China, from SHRIMP U-Pb zircon studies of granitoids: Ore Geology Review, v. 13, p. 275–291.

Wang, X.M., Zhang, R.Y., and Liou, J.G., 1995, UHPM terrane in east central China, *in* Coleman, R., and Wang, X., eds., Ultrahigh pressure metamorphism: London, Cambridge University Press, p. 356–390.

Wang, Y.M., Gao, Y.S., Han, H.M., and Wang, X.H., 2003, Practical handbook of reference materials for geoanalysis: Beijing, Geological Publishing House, p. 16–23 (in Chinese).

Whalen, J.B., Currie, K.L., and Chappell, B.W., 1987, A-type granites: Geochemical characteristics, discrimination and petrogenesis: Contributions to Mineral and Petrology, v. 95, p. 407–419.

Williams, H.M., Turner, S.P., Pearce, J.A., Kelley, S.P., and Harris, N.B.W., 2004, Nature of the source regions for post-collisional, potassic magmatism in southern and northern Tibet from geochemical variations and inverse trace element modeling: Journal of Petrology, v. 45, p. 555–607.

Wright, J.B., 1969, A simple alkalinity ratio and its application to questions of non-orogenic genesis: Geological Magazine, v. 101, p. 3703–84.

Xie, Z., Li, Q.Z., and Gao, T.S., 2006, Comment on "Petrogenesis of post-orogenic syenites in the Sulu Orogenic Belt, East China: Geochronological, geochemical, and Sr-Nd isotopic evidence" by Yang et al.: Chemical Geology, v. 235, p. 191–194.

Xu, J.W., and Zhu, G., 1994, Tectonic models of the Tan-Lu fault zone, eastern China: International Geology Review, v. 36, p. 771–784.

Yan, G.H., Mou, B.L., and Xu, B.L., 2002, Geochronology and Nd-Sr-Pb isotopic characteristics of the Phanerozoic alkali-rich intrusive rocks in northern China and their implication: Geological Review, v. 48, p. 69–75 (in Chinese with English abstract).

Yan, J., Chen, J.F., Yu, G., Qian, H., and Zhou, T.X., 2003, Pb isotopic characteristics of Late Mesozoic mafic rocks from the Lower Yangtze Region: Evidence for enriched mantle: Journal of China University of Geosciences, v. 9, p. 195–206 (in Chinese).

Yang, J., Godard, G., Kienast, J.R., Lu, Y., and Sun, J., 1993, Ultrahigh pressure 60 kbar magnesite-bearing garnet peridotites from northeastern Jiasu, China: Journal of Geology, v. 101, p. 541–554.

Yang, J.H., 2000, Age and metallogenic dynamics of gold mineralization in Jiaodong Peninsula, eastern China (in Chinese with English abstract) [Ph.D. thesis]: Institute of Geology and Geophysics, Chinese Academy of Sciences, p. 133.

Yang, J.H., Chung, S.L., Wilde, S.A., Wu, F.Y., Chu, M.F., Lo, C.H., and Fan, H.R., 2005a, Petrogenesis of post-orogenic syenites in the Sulu Orogenic Belt, East China: Geochronological, geochemical, and Sr-Nd isotopic evidence: Chemical Geology, v. 214, p. 99–125.

Yang, J.H., Wu, F.Y., Chung, S.L., Wilde, S.A., Chu, M.F., Lo, C.H., and Song, B., 2005b, Petrogenesis of Early Cretaceous intrusions in the Sulu ultrahigh-pressure orogenic

belt, east China and their relationship to lithospheric thinning: Chemical Geology, v. 222, p. 200–231.

Yin, A., and Ni, S., 1993, An indentation model for the north and south China collision and the development of the Tan-Lu and Honam fault system, eastern Asia: Tectonics, v. 124, p. 801–813.

Zhang, H.F., Sun, M., Zhou, M.F., Fan, W.M., Zhou, X.H., and Zhai, M.G., 2004, Highly heterogeneous Late Mesozoic lithospheric mantle beneath the North China Craton: Evidence from Sr–Nd–Pb isotopic systematics of mafic igneous rocks: Geological Magazine, v. 141, p. 55–62.

Zhang, R.Y., Hirajima, T., Banno, S., Cong, B., and Liou, J.G., 1995, Petrology of ultrahigh-pressure metamorphic rocks in southern Sulu region, eastern China: Journal of Metamorphic Geology, v. 13, p. 659–675.

Zhang, X., Cawood, P.A., Wilde, S.A., Liu, R., Song, H., Li, W., and Snee, L.W., 2003, Geology and timing of mineralization at the Cangshang gold deposit, north-western Jiaodong Peninsula, China: Mineralium Deposite, v. 38, p. 141–153.

Zhao, G., Wang, D., and Cao, Q., 1997, Geochemical features and petrogenesis of Laoshan Granite in east Shandong Province: Geological Journal of China Universities, v. 3, p. 1–15 (in Chinese with English abstract).

Zheng, Y.F., Wang, Z.R., Li, S.G., and Zhao, Z.F., 2002, Oxygen isotope equilibrium between eclogite minerals and its constraints on mineral Sm-Nd chronometer: Geochimica et Cosmochimica Acta, v. 66, p. 625–634.

Zhong, H., Zhu, W.G., Chu, Z.Y., He, D.F., Song, X.Y., 2007, Shrimp U-Pb zircongeochronology, geochemistry, and Nd-Sr isotopic study of contrasting granites in the Emeishan large igneous province, SW China: Chemical Geology, v. 236, p. 112–133.

Zhou, J.B., Zheng, Y.F., and Zhao, Z.F., 2003, Zircon U-Pb dating on Mesozoic granitoids at Wulian, Shandong Province: Geological Journal of China Universities, v. 9, p. 185–194 (in Chinese with English abstract).

Zhou, J.X., Huang, Z.L., and Bao, G.P., 2013, Geological and sulfur-lead-strontium isotopic studies of the Shaojiwan Pb-Zn deposit, southwest China: Implications for the origin of hydrothermal fluids: Journal of Geochemical Exploration, v. 128, p. 51–61.

Zhou, T.H., and Lu, G.X., 2000, Tectonics, granitoids and Mesozoic gold deposits in East Shandong, China: Ore Geology Reviews, v. 16, p. 71–90.

Zhou, X.H., Zhang, G.H., Yang, J.H., Chen, W.J., and Sun, M., 2001, Sr-Nd-Pb isotope mapping of late Mesozoic volcanic rocks across northern margin of North China Craton and implications to geodynamic processes: Geochimica, v. 30, p. 10–23 (in Chinese with English abstract).

Zou, H.B., Zindler, A., Xu, X.S., and Qi, Q., 2000, Major, trace element, and Nd, Sr and Pb isotope studies of Cenozoic basalts in SE China: Mantle sources, regional variations and tectonic significance: Chemical Geology, v. 171, p. 33–47.